

Lubricant Flow and Accumulation on the Slider's Air Bearing Surface in a Hard Disk Drive

Alejandro Rodriguez Mendez^{1)*}, David B. Bogy¹⁾

1) Computer Mechanics Laboratory, Department of Mechanical Engineering, University of California, Berkeley, CA 94720, USA

Abstract: Lubricant accumulation on the slider's surface of a hard disk drive (HDD) has a detrimental effect on its read/write performance. Air flow through the slider-disk clearance moves some of the lubricant from the air bearing surface (ABS) towards the slider's lateral walls where it accumulates. In this article we show by numerical simulations that the lubricant accumulation characteristics are strongly dependent on the slider's flying height, skew angle and ABS design. The lubricant flow on the slider's surface is quantified numerically. Air shear stress, air pressure and disjoining pressure are used as driving forces in the simulations. The lubricant thickness profile and volume evolution are calculated for two states of the hard disk drive: operating and at rest. In the first state, lubricant is driven by air shear stress towards the trailing edge of the slider where it accumulates on the deposit end. In the second state, lubricant from the deposit end flows back into the ABS driven by the action of disjoining pressure. Lubricant accumulation on the four lateral walls of the slider is taken into account. The lateral walls are unfolded to study the flow using a two dimensional lubrication model. The effects of flying height, skew angle and slider design on the accumulation removal of lubricant from the ABS are determined for the two states of the drive.

Keywords: Air Bearings, Lubricant transfer, Head-disk interface, Hard disk drive

*Corresponding author: Alejandro Rodriguez Mendez (email: aleromende@berkeley.edu)

1. Introduction

In order to achieve high recording densities, the air bearing clearance in a hard disk drive (HDD) has been decreased down to around 2 nm [1]. At this ultra-low spacing lubricant from the disk often transfers to the slider's air bearing surface (ABS) forming a molecularly thin film that imposes a significant disturbance on its flying stability [2-15]. Problems such as head instabilities, disk lubricant depletion and increase in head-disk spacing occur when lubricant is present on the ABS [16-25]. Moreover, it is expected that the lubricant transfer from disk to slider will increase with the use of Heat Assisted Magnetic Recording technology, a possible next generation of HDD [26-30]. To avoid this condition, modern sliders should be able to remove the lubricant from the ABS as fast as possible. Hence, it is necessary to have a thorough understanding of lubricant flow behavior and its driving forces.

The lubricant flow and migration dynamics on the ABS has been the subject of several recent investigations [5, 15, 17, 18, 31, 32, 33]. In [15, 31] the pitch moment and air bearing force were calculated numerically when lubricant droplets are located on the slider's air bearing surface. In [32] the lubricant thickness distribution on the ABS was simulated for diverse slider attitudes and designs. In [5] the lubricant migration on the ABS was computed numerically taking into account the evaporation of lubricant from the slider surface. In [17] there was reasonably good agreement between experiments and modeling of lubricant dynamics on the ABS for a slider at rest and during flying. In [18] the contribution of lubricant on the ABS to magnetic spacing was calculated experimentally and compared with numerical simulations.

In this paper, we focus attention on the effects of flying height, skew angle and ABS design on the accumulation characteristics of lubricant on the slider's ABS and lateral walls. Our approach is solely numerical based on two-dimensional lubrication theory. The lubricant

accumulation outside the ABS is studied by unfolding the four lateral walls of the slider, locating them on the same plane with the ABS, then using the two dimensional model mentioned above. Air shear stress, air bearing pressure and disjoining pressure are considered as driving forces in the simulations. The lubricant profile and its volume evolution are calculated for two states of the HDD: operating (flow) and at rest (reflow). In the first state, lubricant is driven by air shear stress towards the trailing edge of the slider where it accumulates on the so-called deposit end. In the second state, lubricant from the deposit end flows back into the ABS driven by the action of disjoining pressure and surface tension. The governing partial differential equation is solved by means of a finite difference numerical scheme. Four different ABS designs are considered in the numerical simulations to compare the lubricant accumulation characteristics between them. The ABS designs with shorter lubricant removal times are indicated.

2. Governing equations

In current HDD's, the thickness of the lubricant film on the disk surface is of the order of 1 nm [34], and of similar order of magnitude on the slider surface when lubricant transfer has occurred [4]. Even though this film consists of only a few molecules across its thickness, the lubricant flow can be well described using continuum theory with a modified (effective) viscosity [35, 36]. This approach yields adequate results when compared with experiments [18]. The value of the effective viscosity can be several orders of magnitude larger or smaller than that of the bulk liquid [37]. Its actual value is strongly dependent on the slider's surface chemistry, roughness and air shear stress intensity. Within the continuum approach, the conditions of operation in a HDD make it possible to use lubrication theory and thus obtain governing equations for the flow on the slider's surface. First, we proceed by applying a mass balance to an infinitesimal control volume of lubricant as shown in figure 1, to obtain the equation,

$$\frac{\partial h}{\partial t} + \frac{\partial q_1}{\partial x_1} + \frac{\partial q_2}{\partial x_2} = 0, \quad (1)$$

where h is the lubricant thickness, q_1 and q_2 are volume flow rates in the x_1 and x_2 directions respectively. Under the lubrication approximation, the lubricant velocity components at the air interface can be written as [38],

$$v_i = \frac{1}{\mu} \tau_i h - \frac{1}{2\mu} \frac{\partial P}{\partial x_i} h^2, \quad (2)$$

where, v_i , μ , P , τ_i are the lubricant velocity in the x_i -direction, effective viscosity, pressure within the lubricant film and the x_i -component of air shear stress, respectively. Here and henceforth $i = 1, 2$. In equation (2) we have assumed a no-slip boundary condition at the slider-lubricant interface.

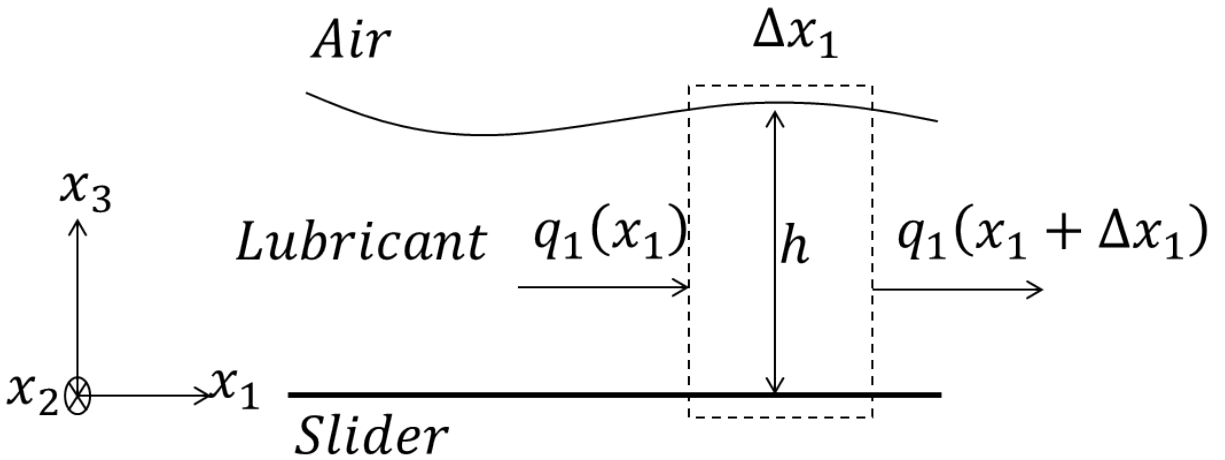


Fig. 1 Control volume depicting the mass balance of lubricant on the air bearing surface.

It is expected that as the film thickness $h \rightarrow 0$, slippage at the interface will have a larger contribution to the overall flow, therefore the assumption of a no-slip condition breaks down. For the thinnest films, slippage can be accounted for by introducing a Navier slip boundary condition

in the model [39]. Here, the velocity at the solid-liquid interface is proportional to the velocity gradient into the liquid. The constant of proportionality is the so-called slip length which is not readily available to us from current literature. Consequently, we simplify the analysis by considering only a zero slip condition in the lubrication model.

The volume flow rates q_i are obtained by integrating (2) across the film thickness,

$$q_i = \int_0^h v_i dx_3 = \frac{1}{2\mu} \tau_i h^2 - \frac{1}{3\mu} \frac{\partial P}{\partial x_i} h^3. \quad (3)$$

Substitution in equation (1) then yields

$$\frac{\partial h}{\partial t} + \sum_{i=1}^2 \frac{\partial}{\partial x_i} \left\{ \frac{1}{2\mu} \tau_i h^2 - \frac{1}{3\mu} \frac{\partial P}{\partial x_i} h^3 \right\} = 0. \quad (4)$$

Equation (4) is the evolution equation for the film thickness h . The pressure P within the lubricant is obtained by a normal stress balance at the air-lubricant interface yielding

$$P = P_a - P_d - P_\gamma, \quad (5)$$

where P_a , P_d , P_γ , are the air, disjoining and surface tension pressures, respectively. The surface tension pressure, also known as Laplace pressure, can be related to the lubricant thickness by [5]

$$P_\gamma = \gamma \left(\frac{\partial^2 (h + h_s)}{\partial x_1^2} + \frac{\partial^2 (h + h_s)}{\partial x_2^2} \right), \quad (6)$$

where γ is the surface tension constant and h_s is the slider's ABS topography as seen in figure 2. It can be shown, either by a non-dimensional analysis or by solving the governing equation (4), that the surface tension effect is negligibly small compared to the other terms in (4). This outcome is also found in [40]. For this reason, the Laplace pressure (6) was not implemented in the following simulations.

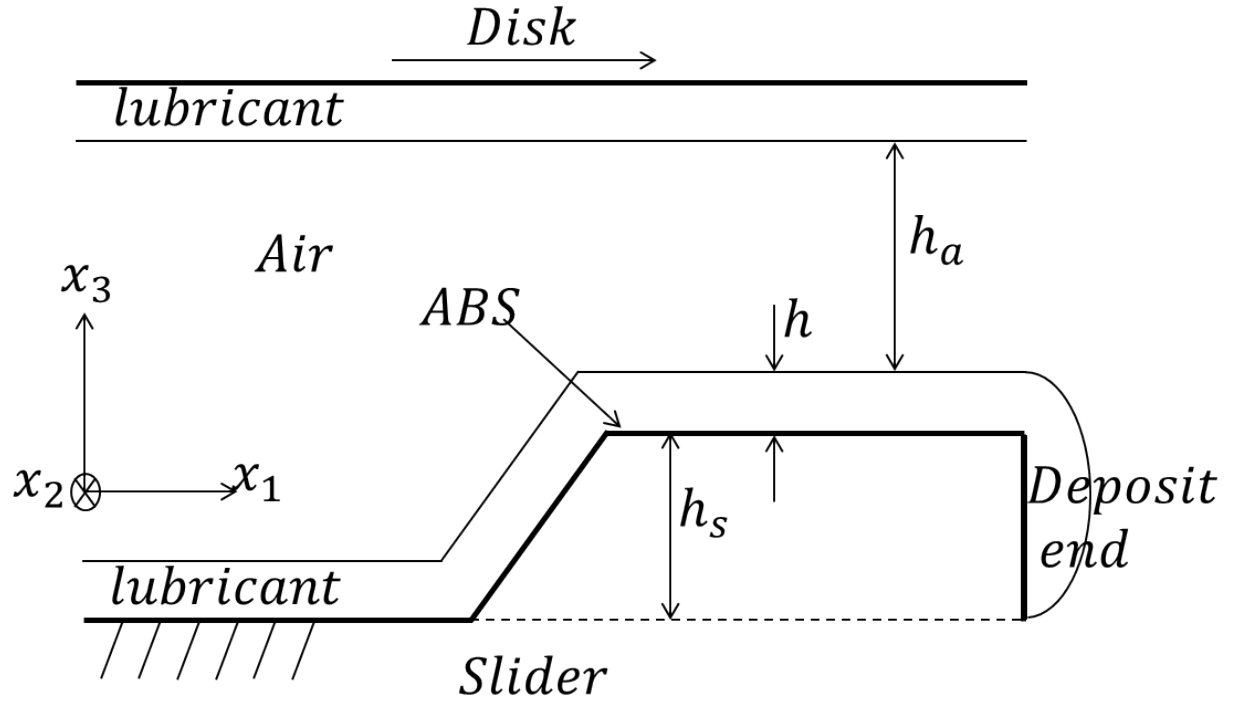


Fig. 2 Sketch of a typical head-disk interface.

For the film characteristics encountered in HDDs the disjoining pressure is expected to be dominated by van der Waals interactions and expressed by [34]

$$P_d = \frac{A}{(h + d_0)^3}, \quad (7)$$

where A is the Hamaker constant that describes the strength of the van der Waals interactions and d_0 is a molecular cutoff distance that accounts for the finite size of the molecules.

There exist an extensive variety of lubricants used in HDDs that differentiate themselves in structural composition, functional end groups and molecular weight. In this paper, the values of the material properties were not chosen to match a specific lubricant. However, the chosen values lie within the range of those lubricant properties commonly found in the available literature. Thus, the calculations were carried out using the material properties: $d_0 = 0.3 \text{ nm}$, $\mu = 0.144 \text{ Pa} \cdot \text{s}$ [36], $A = 5(10^{-20}) \text{ J}$ [41]. The air bearing pressure and air shear stress fields

were calculated using the CMLAir air bearing solver [42]. We assumed that the lubricant on the ABS induces a negligible change in air bearing pressure and air shear stress. Therefore, this calculation was carried out only once for each simulation using a slider with no lubricant. In other words, the air shear and air bearing pressure are considered to be time independent.

3. ABS model and boundary conditions

In order to study the lubricant flow and accumulation outside the ABS using the two dimensional model (4), we unfold the four lateral walls of the slider (walls parallel to the x_3 direction) locating them on the same plane with the ABS as seen in figure 3. By following this approach, the lubricant accumulation on the deposit end as well as on the three other lateral walls can be analyzed.

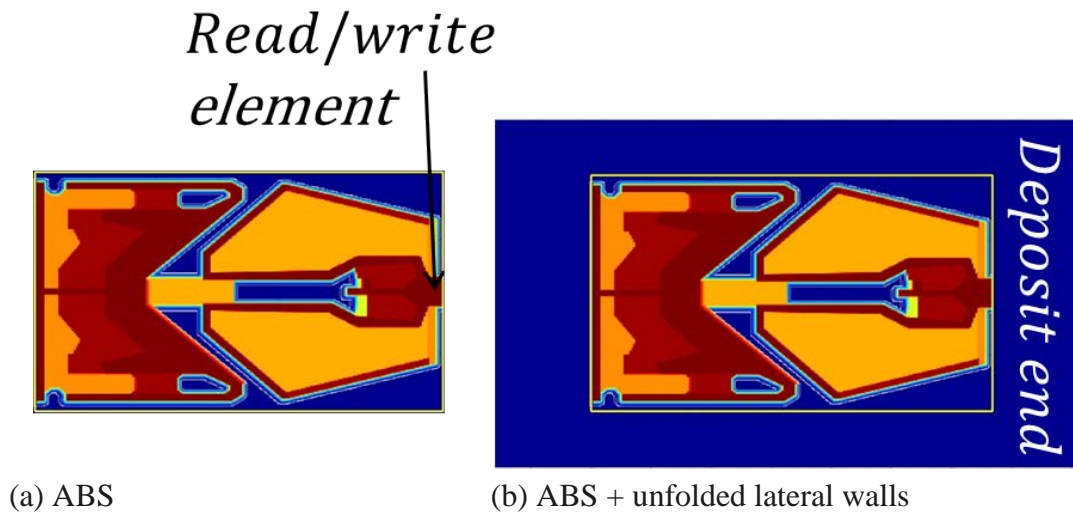


Fig. 3 Slider's (a) ABS design and (b) ABS with unfolded lateral walls.

Zero volume flow rate is imposed as the boundary condition on the four outer edges. The air shear stress and air bearing pressure are set to zero (ambient) outside the actual ABS. With these conditions, the lubricant evolution equation (4) is solved for h using a second order

accurate Crank-Nicolson finite difference scheme [43]. The resulting nonlinear system of equations is solved by a modified Newton's method [44].

4. Results

We simulate the lubricant migration on the surface of a slider with fixed attitude and compare the results with those obtained when its flying height and skew angle are modified. Two states of a HDD are considered: operation (flow) and rest (reflow). Four different slider designs are employed in the simulations. For the initial condition we consider a 1 nm lubricant layer lying uniformly on the slider surface, as seen in figure 4 for $t=0$ s. Under these conditions, the volume on the ABS is calculated as a function of time.

4.1 Fixed attitude

The slider's attitude is fixed at: minimum fly height (FH)=10 nm, skew angle=0°, pitch angle=120 μ rad, roll=0 μ rad. The slider's radial position and disk rotational speed are 18 mm and 5400 rpm, respectively. The simulation results are presented in figure 4. The plots show the lubricant film thickness on the slider surface for selected times. Areas of accumulation are clearly observable inside and outside the ABS. In particular, a relatively large lubricant build up is visible near the center of the deposit end, outside the actual ABS. The film thickness on the read/write element is thinner than that on the rest of the slider; however it could be covered by lubricant due to a reflow process once the HDD is at rest as discussed below. Before discussing the reflow process, it is insightful to analyze the individual contributions to the total flow of the second and third terms in equation (4), namely the Couette flow due to air shear and Poiseuille flow due to pressure gradients within the lubricant respectively. Both terms involve the thickness parameter, h , hence their values change as the lubricant profile evolves with time. To compare

them we compute the ratio of the average magnitude of the Couette term, C , to the average magnitude of the Poiseuille term, P , i.e. C/P . The averages are taken only over the ABS since the air shear stress (hence the Couette term) is assumed zero outside the ABS. The ratio at times $t=0$ s, 10 s, 100 s, 900 s is $C/P= 33.26, 1.10, 0.98, 1.04$ respectively. Thus, we observe that initially, when a flat film covers the slider surface, the shear stress dominates largely the flow process. When the flat film deforms, the contribution of pressure gradients to the flow process become more relevant. For times larger than zero in the above calculations, both terms are approximately of the same order of magnitude. Since the Poiseuille term in (4) consists of disjoining pressure and air bearing pressure, the latter is regarded here as fixed in time, which implies that the disjoining pressure plays a role in the flow process of the same order of importance as the air shear stress.

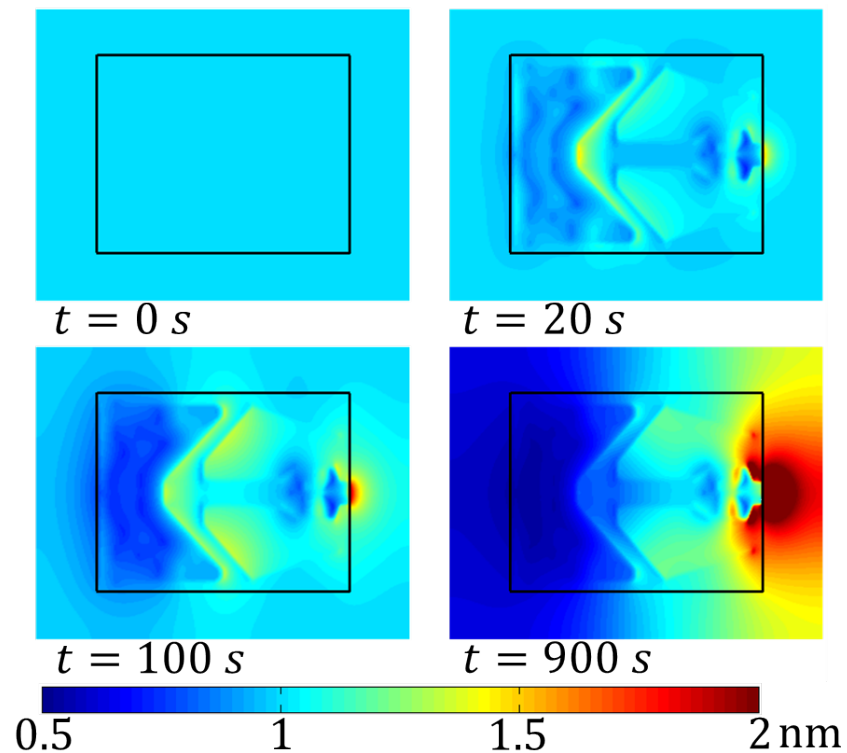


Fig.4 Lube thickness at different times for an operating HDD.

We now simulate the lubricant reflow when the HDD is at rest after 900 s of operation. In this condition, the air bearing pressure and air shear stress are suppressed from the governing equation (4). Here, the lubricant is driven only by the action of disjoining pressure. The simulation results are presented in figure 5. The plots show the lubricant film thickness on the slider surface for selected times during reflow. It is observed from figure 5 that lubricant accumulated on the deposit end diffuses evenly in all directions due to the action of disjoining pressure. This process drives lubricant from the deposit end back into the ABS, contaminating the read/write element. The lubricant continues to diffuse until the film thickness reaches a steady state at approximately $t=3000$ s. The lubricant profile at the final state is almost a uniform film of 1 nm thickness equal to the initial condition shown in figure 4 for $t=0$ s.

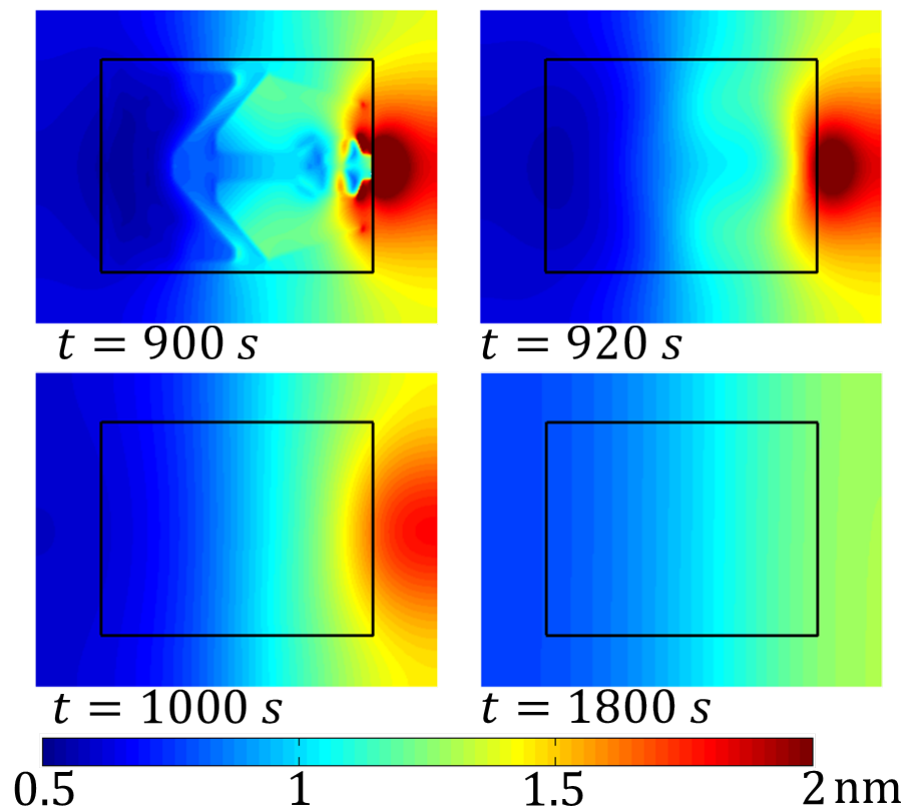


Fig.5 Lubricant thickness profile for a HDD at rest.

4.2 Effect of flying height

The effect of flying height on lubricant flow is now considered. Here, we simulate the film evolution on the slider's surface under the same flying conditions given in the previous section but with minimum flying heights of 10 nm, 50 nm, 100 nm and 150 nm. These values were chosen so as to minimize changes in air bearing pressure and air shear stress due to the migration of lubricant on the ABS since, as discussed in section 2, the air bearing stress and pressure are assumed fixed in time for each simulation. Calculations are performed for the cases of flow and reflow mentioned above. The results are shown in figure 6 where lubricant volume on the ABS is plotted as a function of time. The volume was calculated and normalized only over the actual ABS, i.e. the amount of lubricant on the lateral walls was not included. Therefore, the normalized volume can increase to more than unity due to lubricant from the lateral walls entering into the ABS.

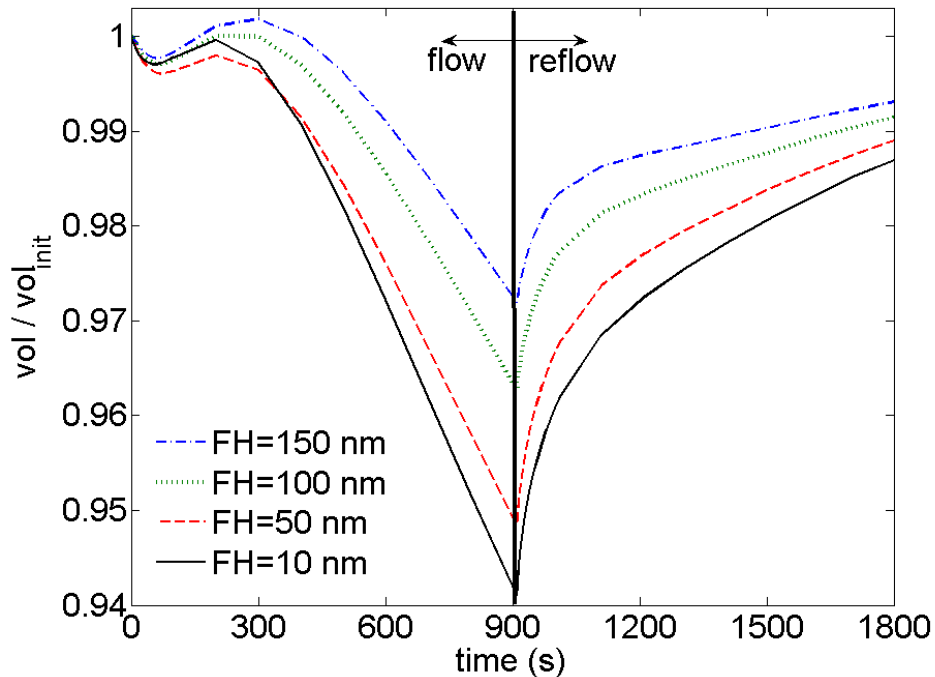


Fig.6 Lubricant volume on the ABS for selected flying heights.

We observe in figure 6 that the volume decreases with time during HDD operations (flow). In this case, lubricant is removed from the ABS mainly by the action of the air shear stress. On the other hand, when the drive is at rest (reflow) the volume increases with time due to lubricant from the deposit end flowing back into the ABS driven by disjoining pressure. It is also observed in figure 6 that a smaller flying height results in a faster lubricant removal during HDD operations. In particular at $t=900$ s, more lubricant is moved out of the ABS as the flying height is reduced. Computing the average air shear stress over the ABS we obtain 127.9 Pa, 111.8 Pa, 98.1 Pa, 88.6 Pa for the minimum flying heights of 10 nm, 50 nm, 100 nm, 150 nm respectively. We note that decreasing the slider's flying height induces an increase in air shear stress that speeds up the lubricant flow process.

4.3 Effect of skew angle

To study the effect of skew angle on the lubricant flow we select the following values of skew angle: 15° , 7° , 0° , -7° , -15° . In this case, the slider's flying attitude is not fixed, i.e. its FH, skew, pitch and roll angles are dependent on the radial position of the slider on the disk. The relation among radial position, skew angle and minimum flying height are given in table 1 for the particular HDD configuration considered in our study.

Table 1. Relation among slider's radial position, skew angle, minimum flying height and average air shear stress.

Radius (mm)	Skew (deg)	min FH (nm)	Air Shear (Pa)
25.254	15	6.849	186.30
21.161	7	7.647	155.00
18	0	9.094	131.23
15.311	-7	10.666	112.31
12.83	-15	11.511	95.91

The simulation results are presented in figure 7. The plots show the lubricant film thickness on the slider's surface for skew angles of 15° , and -15° at time $t=300$ s. It is clear from this figure that one of the effects of skew angle is to mobilize more lubricant towards the sides (top and bottom) of the slider. Moreover, for this particular slider design, the flow process is intensified as the skew angle increases.

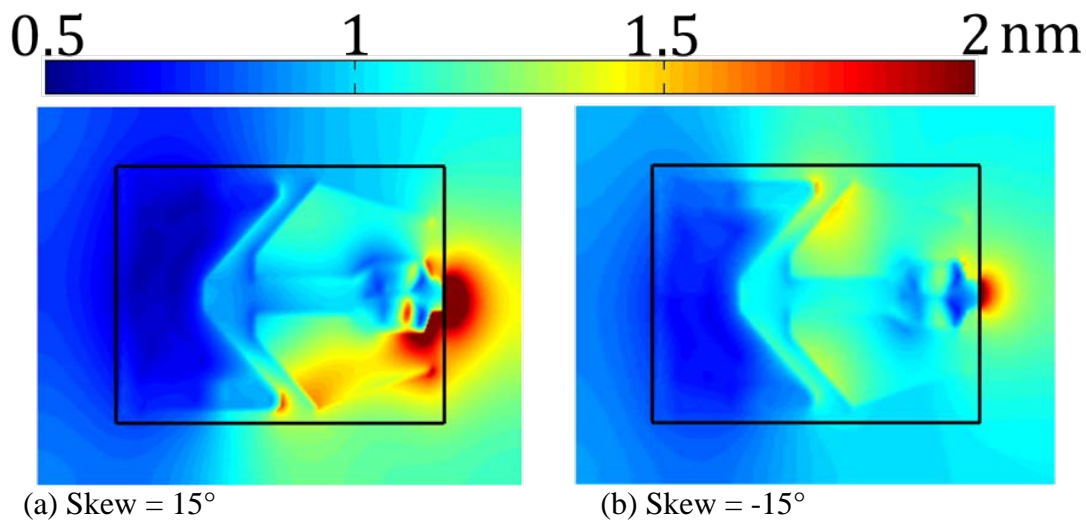


Fig.7 Lubricant profile at $t=300$ s for skew angles of (a) 15° and (b) -15° .

This is observed clearly in figure 8 where the volume of lubricant on the ABS is plotted as a function of time for the selected values of skew angles. The plot shows that, during HDD operations, a faster lubricant removal corresponds to a larger (more positive) value of skew angle, i.e. more lubricant is removed from the ABS as the skew angle increases from negative to positive values.

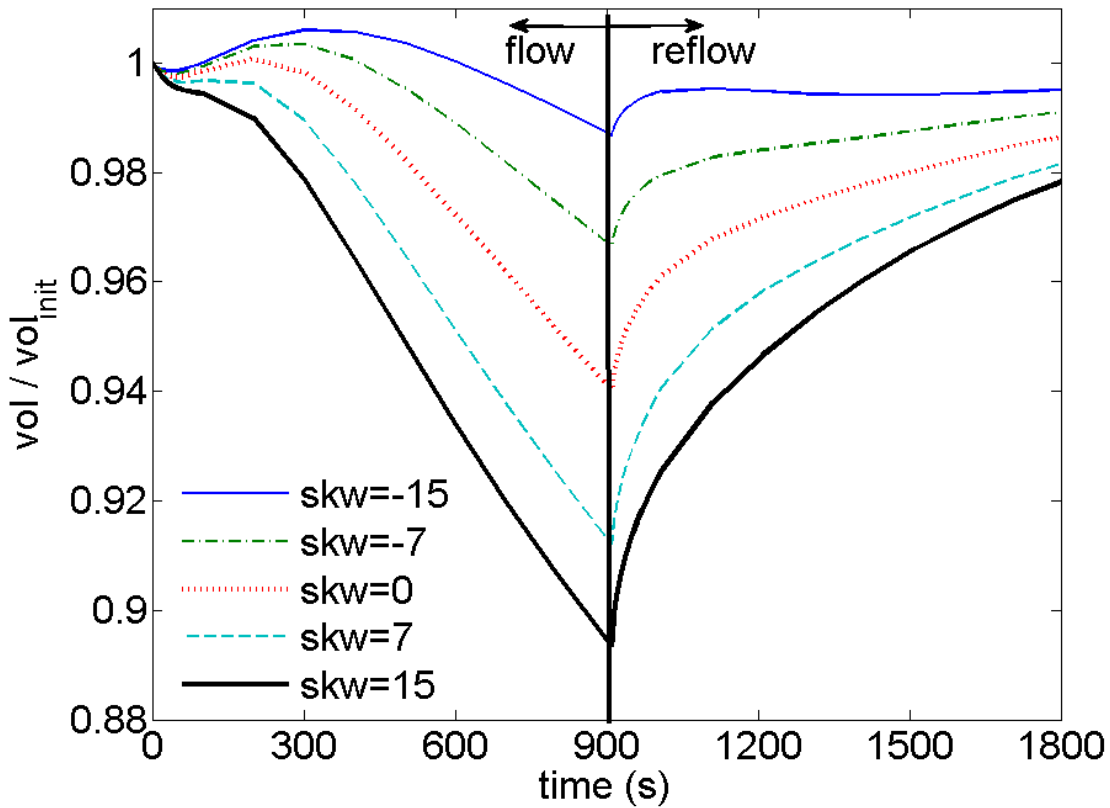


Fig.8 Lubricant volume on the ABS for chosen skew angles.

To explain this behavior, we observe in table 1 that more positive values of skew angle correspond to smaller flying heights (for this particular slider design, figure 3). From table 1, we observe that a reduction in flying height induces an increase in average air shear stress that enhances the flow as discussed in section 4.2.

4.4 Effect of slider design

We analyze the effect of slider design on the lubricant migration process. To this end we choose the four ABS designs presented in the first row of figure 9. The flying attitude of the four sliders is fixed with the same values given in section 4.1. The plots show the lubricant film thickness on the slider surface at times $t=100$ s and $t=900$ s. It is observed that the lubricant

distribution is slider dependent. In particular, at time $t=900$ s, sliders 1 and 4 accumulate a relatively large amount of lubricant near the center of the deposit end, next to the trailing end center pad.

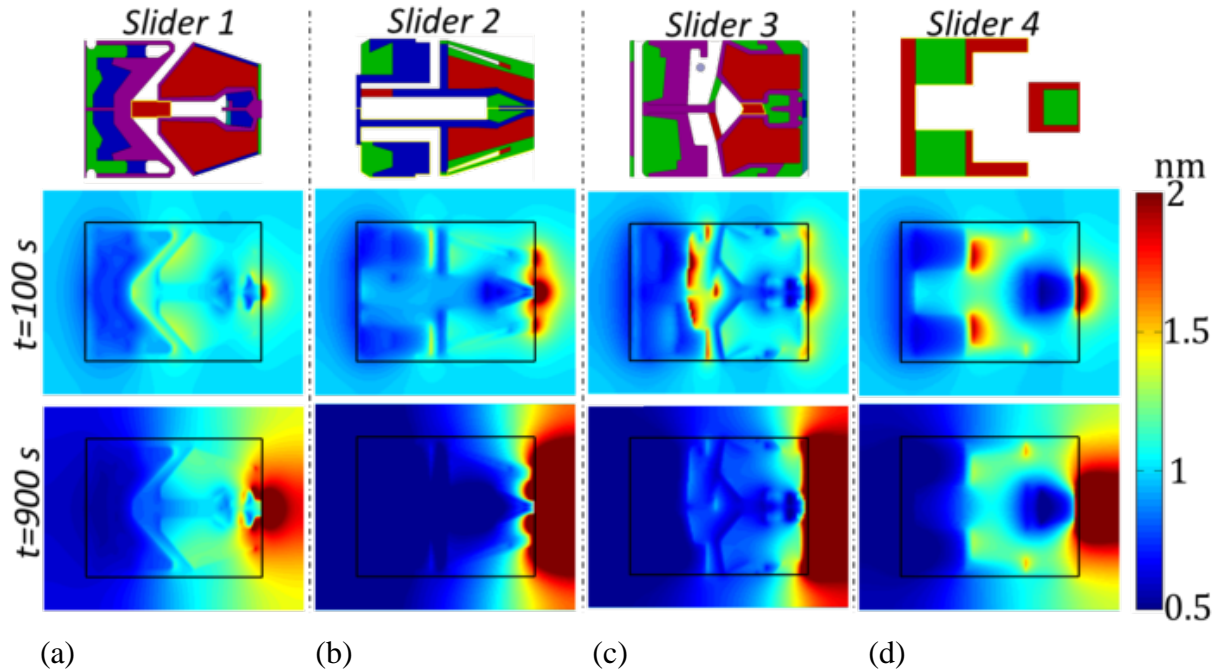


Fig.9 Lubricant thickness profile at times $t=100$ s and $t=900$ s for chosen ABS designs corresponding to: (a) slider 1, (b) slider 2, (c) slider 3, (d) slider 4.

On the other hand, sliders 2 and 3 spread this lubricant across the width (x_2 direction) of the deposit end, i.e. they have a larger area of distribution. The way in which lubricant is accumulated on the deposit end may have implications on how fast the lubricant is removed from the ABS as discussed below.

In figure 10 the lubricant volume on the ABS is plotted as a function of time for the four slider designs. As observed, the curves corresponding to sliders 1 and 4 (and sliders 2 and 3) show similar trajectories, i.e. they are close to each other. Moreover, during HDD operations (flow), sliders 2 and 3 remove more lubricant from the ABS in a shorter period of time than sliders 1 and 4. The average air shear stress over the ABS is 127.9 Pa, 184.3 Pa, 202.4 Pa, and

135.4 Pa for sliders 1, 2, 3 and 4 respectively. We notice that the average air shear stress is larger on sliders 2 and 3 than on sliders 1 and 4. This observation is in agreement with the behavior of the volume plots shown in figure 10, namely that sliders 2 and 3 have a faster clean up time.

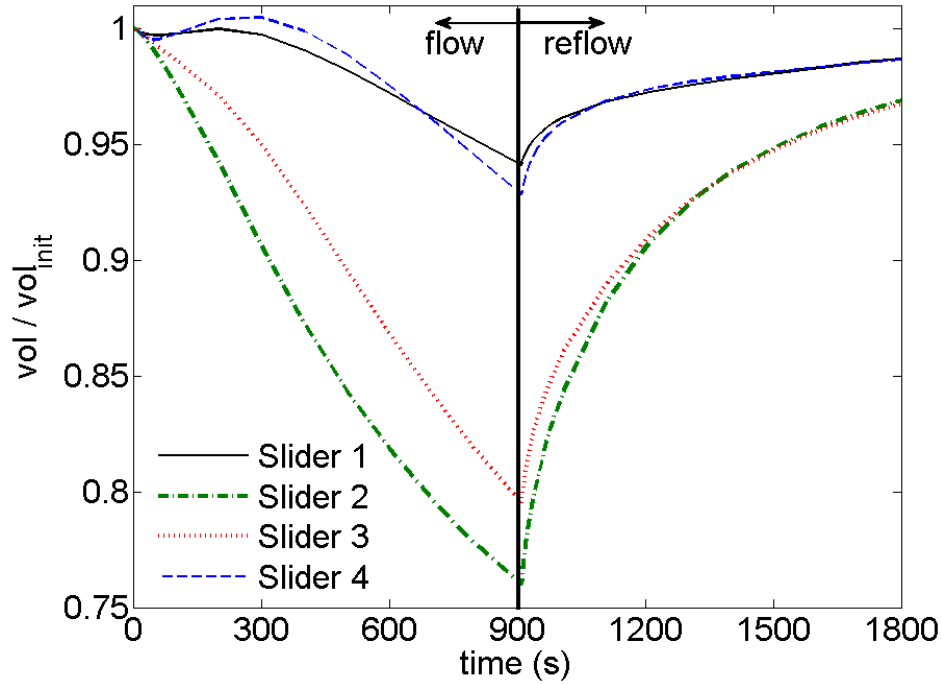


Fig.10 Lubricant volume on the ABS for chosen slider designs.

Since air shearing plays an important role in determining the lubricant flow characteristics, we can gain further insight into the migration process by analyzing the air shear stress profile on the ABS. In figure 11, the vector field and intensity of the air shear stress are plotted for sliders 1 and 3. Besides the fact mentioned above, namely that slider 3 has a larger average shear stress than slider 1, we indicate a few important differences between their shear profiles. In figure 11a, we note that the magnitude of the air shear stress along the trailing end edge of slider 1 is close to zero except on the center pad where it is the largest. From this characteristic, we expect the largest accumulation of lubricant on the deposit end near the center pad, in agreement with the profile shown in figure 9a. Also along this edge we note two regions,

above and below the center pad, where air shear is directed towards the interior of the ABS, i.e. approximately along the $-x_1$ direction. On the other hand, in figure 11b we observe that the air shear stress on the trailing edge of slider 3 is all directed away from the ABS towards the deposit end. Moreover, the shear stress magnitude is relatively large, around 300 Pa, all along the trailing edge and it is the largest on the center pad. Here, we expect a large accumulation to exist all along the trailing end on the deposit end, in agreement with figure 9c.

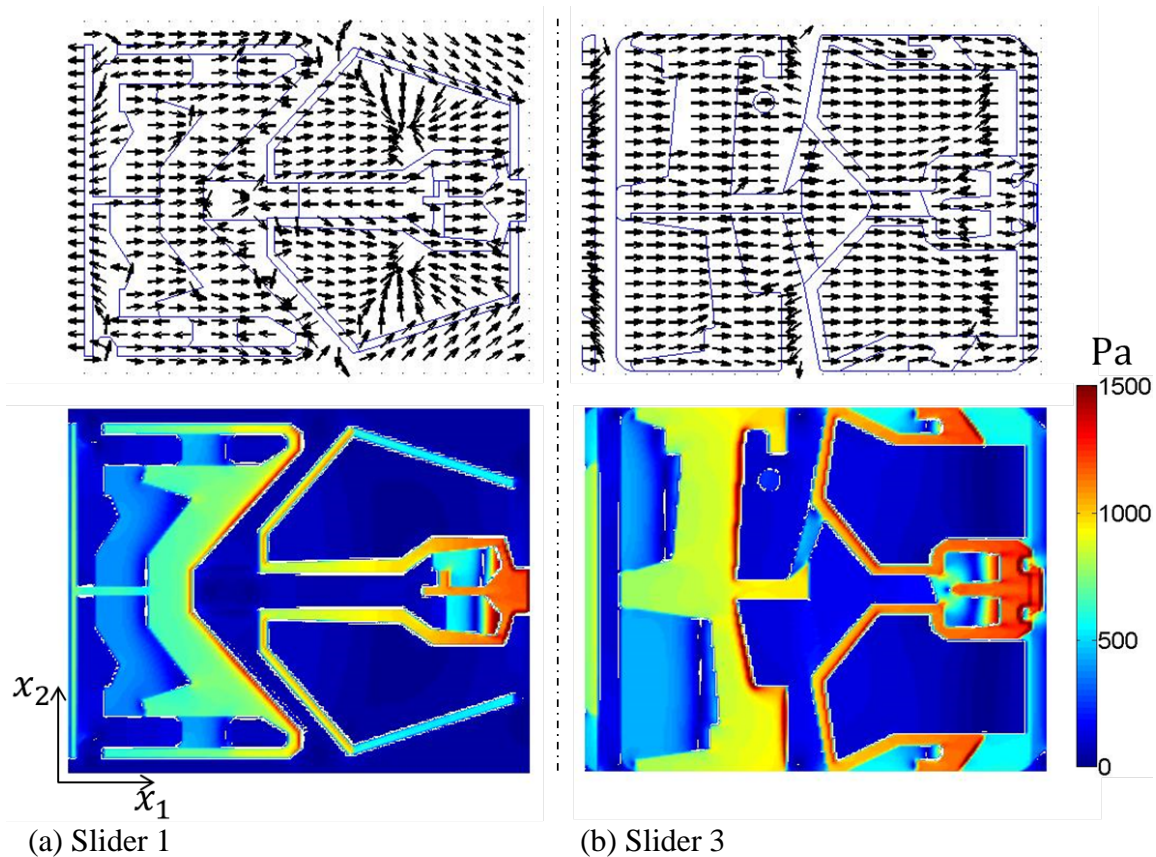


Fig.11 Vector field and magnitude of air shear stress for (a) slider 1 and (b) slider 3.

For the reasons exposed above, it is plausible to relate the time for lubricant removal, on a particular slider design, to the magnitude and distribution of the air shear stress on the ABS. These shear stress characteristics determine the extent of area on the deposit end where most lubricant is accumulated. Therefore, we can use the lubricant accumulation profile on the deposit

end as an indicator of a slider's speed in removing lubricant from the ABS. As it is observed in figure 9a,d accumulation on sliders 1 and 4 occurs largely in a small area near the center of the deposit end and the average magnitude of shear stress is smaller than sliders 2 and 3; therefore lubricant is removed from the ABS at a relatively slow rate which is clearly depicted in figure 10. On the other hand, figure 9b,c shows that accumulation on sliders 2 and 3 occurs all along the trailing edge on the deposit end and the average shear stress is larger than sliders 1 and 4; consequently lubricant is removed from the ABS at a higher rate as demonstrated in figure 10.

5. Conclusions

It is shown that lubricant accumulation characteristics on the slider surface are strongly dependent on the slider's flying height, skew angle and ABS design. The lubricant thickness profile and volume evolution on a slider's ABS are calculated including the effects of air shear stress, air bearing pressure and disjoining pressure as driving forces. Changes in flying height, skew angle and slider design are taken into account in the numerical simulations. It is concluded that a smaller flying height contributes to a faster lubricant removal from the ABS due to an induced increase in air shear stress. It is observed that when the HDD is at rest, lubricant accumulated on the deposit end flows back into the ABS driven by the action of disjoining pressure. It is found, for a particular slider design, that increasing the slider's skew angle has the effect of enhancing the lubricant flow process due to a decrease in the slider's flying height. The lubricant migration process is significantly dependent on the ABS design. It is found that slider designs that accumulate most lubricant on a broader area on the deposit end and have larger values of air shear stress remove lubricant from the ABS at higher volume rates than those designs where accumulation is concentrated near the center of the deposit end and have smaller values of average shear stress.

References

- [1] Marchon, B., Olson, T.: Magnetic spacing trends: from LMR to PMR and beyond. *IEEE Trans. Magn.* **45**(10), 3608-3611 (2009)
- [2] Marchon, B., Karis, T., Dai, Q., Pit, R.: A model for lubricant flow from disk to slider. *IEEE Trans. Magn.* **39**(5), 2447-2449 (2003)
- [3] Tani, H., Iwasaki, K., Maruyama, Y., Ota, I., Tagawa, N.: Lubricant pickup of ultra-thin PFPE lubricants with different backbone structures. *IEEE Trans. Magn.* **47**(7), 1837-1841 (2011)
- [4] Tani, H., Kubota, M., Tsujiguchi, Y., Tagawa, N.: Visualization of lubricant pickup phenomena by lubricant thickness mapping on slider surface. *Microsyst. Technol.* **17**, 1175-1178 (2011)
- [5] Wu, L.: A model for liquid transfer between two approaching gas bearing surfaces through coupled evaporation-condensation and migration dynamics. *J. Appl. Phys.* **104**(1), 014503 (2008)
- [6] Li, J., Xu, J., Aoki, Y.: Air bearing design to prevent reverse flow from the trailing edge of the slider. *Tribol. Lett.* **35**(2), 113-120 (2009)
- [7] Kasai, P. H., Raman, V.: Lubricant transfer in disk drives. *Tribol. Lett.* **48**(3), 367-374 (2012)
- [8] Kim, S. H., Dai, Q., Marchon, B., Flechsig, K.: Humidity effects on lubricant transfer in the head-disk interface of a hard disk drive. *J. Appl. Phys.* **105**(7), 07B704 (2009)
- [9] Ma, Y., Tan, B. K., Liu, B.: Lubricant transfer and slider-lubricant interaction at ultra-low flying height. *J. Magn. Magn. Mater.*, **303**(2), e110-e114 (2006)

- [10]Tan, B. K., Liu, B., Ma, Y., Zhang, M., Ling, S. F.: Effect of electrostatic force on slider-lubricant interaction. *IEEE Trans. Magn.* **43**(6), 2241-2243 (2007)
- [11]Kubotera, H., Imamura, T.: Monte Carlo simulations of air shielding effect on lubricant transfer at the head disk interface. *Appl. Phys. Lett.* **94**(24), 243112 (2009)
- [12]Smallen, M. J., Huang, H. W.: Effect of disjoining pressure on disk-to-head lubricant transfer. *IEEE Trans. Magn.* **39**(5), 2495-2497 (2003)
- [13]Ma, Y., Liu, B.: Lubricant transfer from disk to slider in hard disk drives. *Appl. Phys. Lett.* **90**(14), 143516 (2007)
- [14]Ma, Y., Liu, B.: Dominant factors in lubricant transfer and accumulation in slider-disk interface. *Tribol. Lett.* **29**(2), 119-127 (2008)
- [15]Wu, L.: Modeling and simulation of the interaction between lubricant droplets on the slider surface and air flow within the head/disk interface of disk drives. *IEEE Trans. Magn.* **42**(10), 2480-2482 (2006)
- [16]Ambekar, R. P., Bogy, D. B., Bhatia, C. S.: Lubricant depletion and disk-to-head lubricant transfer at the head-disk interface in hard disk drives. *Journal of tribology*, **131**(3) (2009)
- [17]Marchon, B., Guo, X. C., Moser, A., Spool, A., Kroeker, R., Crimi, F.: Lubricant dynamics on a slider: "The waterfall effect". *J. Appl. Phys.* **105**(7), 074313 (2009)
- [18]Mate, C. M., Marchon, B., Murthy, A. N., Kim, S. H.: Lubricant-induced spacing increases at slider–disk interfaces in disk drives. *Tribol. Lett.* **37**(3), 581-590 (2010)
- [19]Ambekar, R. P., Bogy, D. B.: Effect of slider lubricant pickup on stability at the head-disk interface. *IEEE Trans. Magn.* **41**(10), 3028-3030 (2005)

- [20]Ambekar, R., Gupta, V., Bogy, D. B.: Experimental and numerical investigation of dynamic instability in the head disk interface at proximity. *Journal of tribology*, **127**(3), 530-536 (2005)
- [21]Matsuoka, H., Kan-Nen, M., Fukui, S.: Theoretical model for lubricant pick-up (Breakage of liquid meniscus bridge due to elongation in bridged direction). *IEEE Trans. Magn.* **47**(10), 3582-3585 (2011)
- [22]Marchon, B.: Lubricant design attributes for subnanometer head-disk clearance. *IEEE Trans. Magn.* **45**(2), 872-876 (2009)
- [23]Gui, J., & Marchon, B.: Fly/stiction: mechanical instability of a head-disc interface. *IEEE Trans. Magn.* **34**(4), 1804-1806 (1998)
- [24]Cong, P., Kubo, T., Nanao, H., Minami, I., Mori, S.: Tribological performance and transfer behavior of lubricating oils at head-disk interface under volatile organic contamination. *Tribol. Lett.* **19**(4), 299-309 (2005)
- [25]Pit, R., Zeng, Q. H., Dai, Q., Marchon, B.: Experimental study of lubricant-slider interactions. *IEEE Trans. Magn.* **39**(2), 740-742 (2003)
- [26]Ma, Y., Liu, B.: Lube depletion caused by thermal-desorption in heat assisted magnetic recording. *IEEE Trans. Magn.* **44**(11), 3691-3694 (2008)
- [27]Dahl, J. B., Bogy, D. B.: simulation of lubricant recovery after heat-assisted magnetic recording writing. *Tribol. Lett.* **52**(1), 163-174 (2013)
- [28]Ji, R., Dao, T. K. L., Xu, B. X., Xu, J. W., Goh, B. L., Tan, E., Xie, H. Q., Liew, T.: Lubricant Pickup Under Laser Irradiation. *IEEE Trans. Magn.* **47**(7), 1988-1991 (2011)
- [29]Wu, L.: Modelling and simulation of the lubricant depletion process induced by laser heating in heat-assisted magnetic recording system. *Nanotechnology*, **18**(21), 215702 (2007)

- [30]Zhang, J., Ji, R., Xu, J. W., Ng, J. K. P., Xu, B. X., Hu, S. B., Yuan, H. X., Piramanayagam, S. N.: Lubrication for heat-assisted magnetic recording media. *IEEE Trans. Magn.* **42**(10), 2546-2548 (2006)
- [31]Wu, L.: A two-dimensional model for the interaction between lubricant droplet on the slider surface and air flow within the head/disk interface of disk drives. *J. Appl. Phys.* **99**(8), 08N101 (2006)
- [32]Kubotera, H., Bogy, D. B.: Lubricant migration simulations on the flying head slider air-bearing surface in a hard disk drive. *IEEE Trans. Magn.* **43**(9), 3710-3715 (2007)
- [33]Liu, N., Bogy, D. B.: Air-bearing shear force in the head-disk interface of hard disk. *Tribol. Lett.* **35**(2), 121-125 (2009)
- [34]Mate, C. M.: Taking a fresh look at disjoining pressure of lubricants at slider-disk interfaces. *IEEE Trans. Magn.* **47**(1), 124-130 (2011)
- [35]Scarpulla, M. A., Mate, C. M., Carter, M. D.: Air shear driven flow of thin perfluoropolyether polymer films. *J. Chem. Phys.* **118**, 3368-3375 (2003)
- [36]Marchon, B., Dai, Q., Nayak, V., Pit, R.: The physics of disk lubricant in the continuum picture. *IEEE Trans. Magn.* **41**(2), 616-620 (2005)
- [37]Mate, C. M.: Spreading kinetics of lubricant droplets on magnetic recording disks. *Tribol. Lett.* **51**, 385-395 (2013)
- [38]Batchelor, G. K.: *An introduction to fluid dynamics*. Cambridge university press (2000)
- [39]O'Brien, S. B. G., Schwartz, L. W.: Theory and modeling of thin film flows. *Encyclopedia of surface and colloid science*, 5283-5297 (2002)

- [40] Kubotera, H., Bogy, D. B.: Numerical simulation of molecularly thin lubricant film flow due to the air bearing slider in hard disk drives. *Microsyst. Technol.* **13**(8-10), 859-865 (2007)
- [41] Bowles, A. P., Hsia, Y. T.: Quasi-equilibrium AFM measurement of disjoining pressure in lubricant nanofilms II: Effect of substrate materials. *Langmuir*, **25**(4), 2101-2106 (2009)
- [42] http://cml.berkeley.edu/cmlair_new.html
- [43] LeVeque, R. J.: *Finite difference methods for ordinary and partial differential equations: steady-state and time-dependent problems.* Siam (2007)
- [44] Cha, E. T.: *Numerical analysis of head-disk assembly dynamics for shaped-rail sliders with sub-ambient pressure regions.* University of California, Berkeley (1993)